



# Comparative study of AZO and ITO thin film sputtered at different temperatures and their application in $\text{Cu}_2\text{ZnSnS}_4$ solar cells

Yilei Lu<sup>1</sup> · Shurong Wang<sup>1,2</sup> · Min Yang<sup>1</sup> · Xin Xu<sup>1</sup> · Qi Li<sup>1</sup>

Received: 1 May 2018 / Accepted: 9 August 2018 / Published online: 3 September 2018  
© Springer Science+Business Media, LLC, part of Springer Nature 2018

## Abstract

Indium tin oxide (ITO) and Al-doped ZnO (AZO) are the most common materials for transparent conducting films used as a front contact layer on solar cells. In this study, AZO and ITO thin films were deposited by sputtering under different temperatures in order to study the difference between two kinds of thin films in crystal structure, morphology, optical and electrical properties. In the same time, CZTS solar cells were also fabricated using AZO or ITO thin films as the window layers, and the obtained highest efficiencies of 3.66% and 5.12% are based on AZO and ITO window layers with different sputtering temperatures, respectively.

## 1 Introduction

Transparent conducting oxide films were widely used in the kesterite solar cell as the windows layer. In recent years, the most common materials are Al doped zinc oxide (AZO) and indium tin oxide (ITO) because they both have advantages of comparable high optical transmittance, non-toxicity and low electrical resistivity [1, 2]. More in deeply, the conductive mechanism of these two films is similar. The low electrical resistivity of ITO films is due to the large concentration of oxygen vacancies, interstitial atom in exist in the lattice and substitutional tin dopants. Meanwhile, the conductive mechanism of AZO films is due to oxygen vacancies and substitutional Al dopants. In laboratory, usually these materials are prepared by different methods such as magnetron sputtering [3], sol–gel method [4], electron-beam evaporation [5] and chemical vapor deposition [6].

Currently, the champion efficiency of CZTSSe solar cell is still 12.6% and 50 nm ITO was used as windows layer [7]. IREC group fabricated  $\text{Cu}_2\text{ZnSnGeSe}_4$  solar cell with efficiency of 10.6% and usually used ITO as windows layer [8]. Meanwhile, AZO films were used in the 8.4% efficiency of CZTS solar cell [9] and the 10.4% efficiency of CZTSe solar cell was fabricated by Li et al. [10]. However, these articles are less about the detail research of windows layer. Up to now, the effect of the RF sputtering power on micro-structural, optical and electrical properties of Al doped ZnO thin films has been investigated [11]. Moreover, an interest research about AZO film was deposited on ITO precursor on glass substrate by DC magnetron sputtering was also reported [12].

In this work, we deposited the AZO and ITO thin films by sputtering at different temperatures in order to study the difference between two kind of thin films in crystal structure, morphology, optical and electrical properties. Furthermore, we use these thin films as the windows layers of CZTS solar cells by using magnetron sputtering. Finally, the CZTS solar cells were fabricated by conventional method and the obtained highest efficiencies of 3.66% and 5.12% are based on AZO and ITO windows layers with different sputtering temperatures, respectively.

---

**Electronic supplementary material** The online version of this article (<https://doi.org/10.1007/s10854-018-9853-y>) contains supplementary material, which is available to authorized users.

---

✉ Shurong Wang  
shrw88@aliyun.com

<sup>1</sup> Key Laboratory of Rural Energy Engineering in Yunnan Province, Yunnan Normal University, Juxian street no. 768, Kunming 650500, People's Republic of China

<sup>2</sup> Yunnan Key Lab of Opto-electronic Information Technology, Yunnan Normal University, Kunming 650500, People's Republic of China

## 2 Experimental details

### 2.1 Preparation of thin films

AZO and ITO thin films were deposited on glass substrate by RF magnetron sputtering. AZO or ITO with 76.2 mm diameter were kept at a distance of 100 mm from substrate. The 99.99% pure Ar gas was used as gas. The substrate was rotated at 5 rpm and the deposition was carried out at working pressure of 0.3 Pa. AZO and ITO thin films were deposited at temperatures of RT, 50 °C, 100 °C, 150 °C, 200 °C, 250 °C, 300 °C, 350 °C, 400 °C, 450 °C and 500 °C at constant RF power of 80W. AZO and ITO thin films thickness were around 147–260 and 287–328 nm. It should be noted that AZO and ITO thin films had the same deposition time of 60 min.

The characterization of thin films prepared by different substrate temperatures were performed with variety of measuring tools. The structural analysis was done by X-ray diffraction (XRD) using a Rigaku Ultima IV diffractometer with Cu K<sub>α</sub> radiation at 40 kV and 40 mA. The morphology of the films was examined by field emission scanning electron microscopy (FESEM Carl Zeiss SUPRA 55VP) at 5KV. The optical and electrical properties of the films were measured by using a UV–VIS–NIR spectrophotometer (UV-3600) and Hall measurement, respectively.

### 2.2 Preparation of CZTS films and solar cells

Mo back layer was deposited on 10×10 cm<sup>2</sup> soda-lime glass by DC-magnetron sputtering deposition using 99.99% purity targets. The sputtering condition is 180W DC power under room temperature and 1.6–0.3 Pa working pressure. The precursors were deposited by sputtering 99.99% CuSn alloy target and 99.99% Zn target using RF and DC power. The substrate was rotated at 7 rpm and deposition was made at room temperature. Then, the preparation of CZTS film absorber is divided into two steps: the first step is soft alloy that the precursor samples were annealed in a tubular furnace capable of working in vacuum and inert gas atmosphere. The alloying temperature was 250 °C with heating rate of 25 °C min<sup>-1</sup> and holding time was 30 min. For the second step, the alloyed precursors were put into a graphite box and annealed at 560 °C for 20 min using sulfur powder as sulfur source under 3000 Pa Ar atmosphere. After that the CZTS film samples were cooled down to room temperature naturally. Solar cells based on the CZTS films were fabricated by depositing CdS buffer layer

with thickness about 60 nm using chemical bath deposition method, followed by sputtering a 50 nm i-ZnO layer and AZO and ITO windows layer under different substrate temperatures. Finally, the Ni–Al front electrodes were deposited by thermal evaporation. The J–V measurements were performed by using a solar simulator equipped with an AM1.5G filter and a Keithley 2400 sourcemeter. The one-Sun intensity (100 mw cm<sup>-2</sup>) was calibrated with a Si reference cell.

## 3 Results and discussion

AZO and ITO thin films were deposited by RF magnetron sputtering at different substrate temperatures. The thickness of these thin films are shown in Table 1 and Supplementary figure S1. It should be noted that no matter AZO or ITO, the thickness of the films increases with the increase of substrate temperatures. This can be explained that the higher substrate temperature contributes to the improvement of deposition rate [13]. Furthermore, the energy of vapor deposition is very large in magnetron sputtering, and it is possible to cause a certain chemical bond fracture reorganization process on the substrate surface [14]. In the process of increasing the substrate temperature, the chemical adsorption reaction process is accelerated, owing to the substrate temperature is still in a small range that can not make the chemisorption of the atomic re-evaporation rate increase, thus increasing the deposition rate.

XRD was used to study the effect of different substrate temperature on the crystal structure, Fig. 1 represents the XRD patterns of AZO and ITO thin films sputtered at different temperatures. Figure 1, 1 showed that AZO thin films had a polycrystalline wurtzite structure and consisted of hexagonal crystallites with a preferred orientation in the (002) directions. Meanwhile, the (103) orientation was also observed and the secondary (101), (102) plane reflections were present in 350–500 °C samples. At temperature of 150 °C, low intense (103) peak and well crystalline (002) peak of AZO were observed. When temperature was decreased to RT~100 °C, the intensity of (002) peak diminishes dramatically and (103) peak grows slightly. When temperature was increased to 200–450 °C, the intensity of (002) peak decreases to varying degrees and (103) peak grows clearly. Interestingly, when temperature reached to 500 °C, the XRD pattern is similar to the RT~100 °C samples. When the temperature was increased, the XRD peaks in AZO shift to higher 2 theta, because higher substrate temperature increases crystal quality. The Full Width at Half Maximum (FWHM) is range from 0.424 to 1.38, which indicated that the grain size of the 400 °C sample is larger

**Table 1** The thickness of AZO and ITO thin film sputtered at different temperatures

Samples (nm)	RT	50 °C	100 °C	150 °C	200 °C	250 °C	300 °C	350 °C	400 °C	450 °C	500 °C
AZO	147	158.3	169.5	180.8	192.1	203.4	214.7	225.9	237.2	248.5	259.8
ITO	287	290.9	295	299	303.1	307.2	311.3	315.4	319.4	323.5	327.6

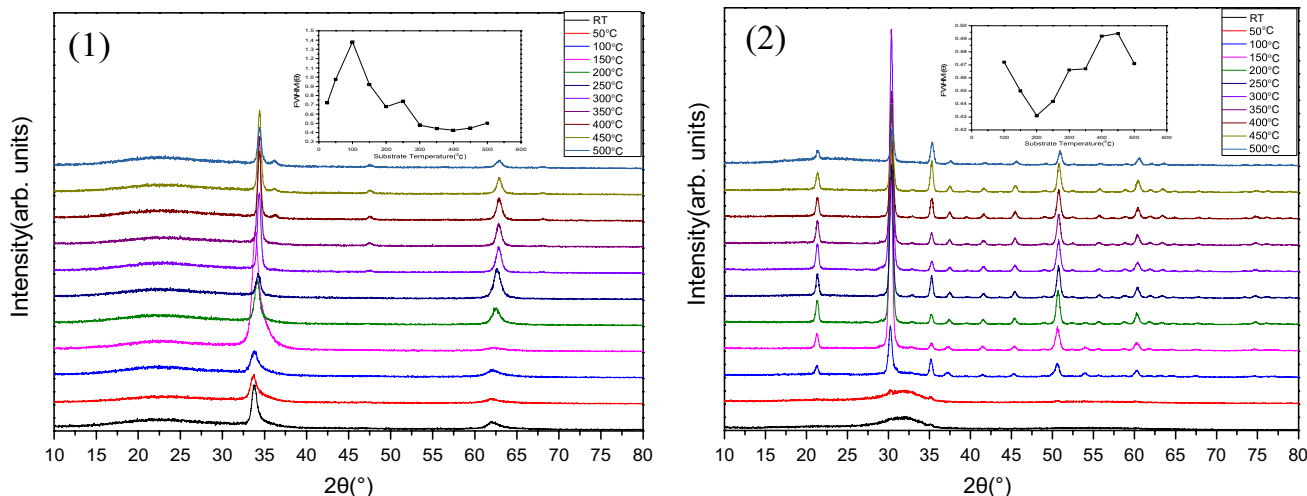


Fig. 1 XRD patterns of the 1 AZO and 2 ITO thin films obtained by the different substrate temperatures

than the other samples, according to the Scherrer formula. For ITO thin films, the different from AZO is that the structure of RT and 50 °C is amorphous. It can be seen that the samples from 100 to 500 °C show plans corresponding to (211), (222), (400), (440), (622), which are related to the structure of cubic  $In_2O_3$  phase. The intensity of (222) peak increased obviously for 100 °C to 200 °C samples, however the intensity of 250 °C samples decreased slightly. At the temperature of 300 °C, the strongest intense (222) peak of ITO were observed. For 350–500 °C samples, as the temperature rising the intensity of (222) peak decreased continuously. The different from AZO films is that the FWHM of ITO films is range from 0.431 to 0.494, which showed that the FWHM of each samples and crystalline quality are very close.

The transmittance spectra for AZO and ITO films sputtered at different temperatures were measured in Fig. 2. It is clearly observed from Fig. 2a that with increase in the deposition temperature the transmission values of AZO films decreases. Kumar et al. suggested that the reduction in the transmittance can be attributed to the increase in the metal to oxygen ratio (Zn/O) causing an increase in the carrier density [15]. The mean transmission of all the AZO thin films was approximately 85% and the highest transmission was attained for the AZO film deposited at 150 °C. The transmission of ITO thin films in the visible light range increased at beginning and then decreased with increasing substrate temperatures which was showed in Fig. 2b. The mean transmission of the ITO thin films was approximately

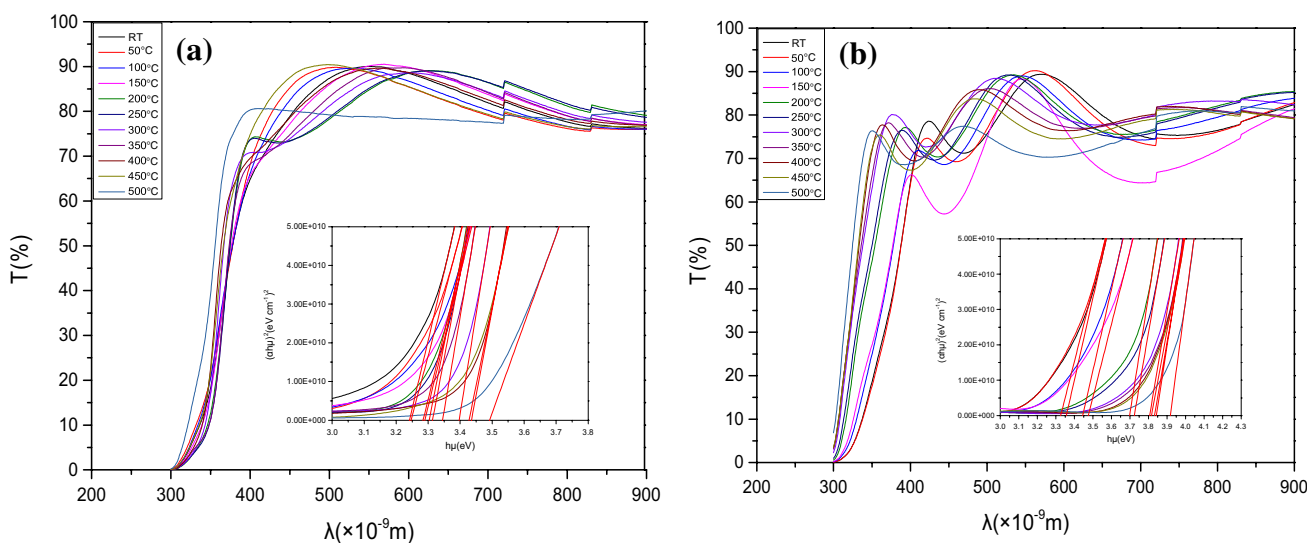


Fig. 2 The transmittance spectra and optical band gap of a AZO and b ITO thin films prepared by the different substrate temperatures

80% and the highest transmission was attained for the ITO film deposited at 50 °C. By measuring the transmittance (T) and reflectance (R) of the AZO and ITO thin films, the optical absorption coefficient ( $\alpha$ ) of the AZO and ITO thin films is given by the equation [16]:

$$\alpha = \frac{1}{d} \left[ \frac{(1-R)^2}{T} \right] \quad (1)$$

where (d) is the thickness of thin films. The optical band gap energy is obtained by the following equation [16]:

$$\alpha h\nu = A(h\nu - E_g) \quad (2)$$

where  $\alpha$  is the optical absorption coefficient, A is a constant,  $E_g$  is the band gap energy. An interesting phenomenon can be found that with increase in the substrate temperature the optical band gap energies of AZO and ITO films increase, so that the windows layer materials with different bandgap can be obtained by different sputtering temperatures. In general, the optical band gap energies of AZO and ITO films were ranged from 3.28 to 3.48 eV and 3.33–3.92 eV which showed in Fig. 2a, b.

Figure 3 presented the electrical properties, including the mobility, carrier concentration and electrical resistivity, of the AZO thin films (a) and ITO thin films (b) at various substrate temperatures. It can be observed from Fig. 3a that the resistivity of AZO thin films increased at first, and then it decreased as the substrate temperature increased from 50 to 500 °C. The Hall measurements indicated that the AZO thin film deposited at 300 °C had the relatively higher electron density and mobility. Thus, the decrease in resistivity is due to the increased mobility and carrier concentration because the resistivity is proportional to the reciprocal of the value of mobility and carrier concentration. Figure 3b

showed that the resistivity of ITO thin films increased as the substrate temperature increased from RT to 150 °C, and then decreased. The Hall measurements indicated that the ITO thin film deposited at 400 °C had the relatively higher electron density and mobility. The mobility in the ITO film is affected by crystallization and the carrier concentration depends on the Sn dopant or the number of oxygen vacancies [17]. When the substrate temperature reaches to 350 °C, the value of carrier concentration decreased obviously. This may be the higher temperature will introduce oxygen into ITO thin film, which will decrease the number of oxygen vacancies. As a result, it is unsuitable if the substrate temperature is too high for fabricating ITO thin films. Above all, the lowest resistivity of AZO thin films was  $1.57 \times 10^{-2} \Omega \text{ cm}$  for the temperature of 300 °C, the carrier concentration and mobility were  $8.4 \times 10^{19} \text{ cm}^{-3}$  and  $4.76 \text{ cm}^2 \text{ V}^{-1} \text{ s}^{-1}$ . And the lowest resistivity of ITO thin films was  $1.5 \times 10^{-4} \Omega \text{ cm}$  for the temperature of 400 °C, the carrier concentration and mobility were  $1.24 \times 10^{21} \text{ cm}^{-3}$  and  $32.8 \text{ cm}^2 \text{ V}^{-1} \text{ s}^{-1}$ , respectively.

In order to find out the reason of ITO films and AZO films with different electrical and optical properties, the surface morphologies of the thin films were investigated. Figure 4a–d shows the surface morphology of the ITO films deposited at different substrate temperatures. Obviously, the surface morphology of the ITO films changed with increasing substrate temperatures. At the beginning, the ITO film deposited at RT has a smooth surface with round-shaped grains. As the substrate temperature increased, the crystallinity and grain size of the ITO films were significantly improved. When the substrate temperature was 300 °C, the ITO film exhibited a relatively large grain size and regular “petal” shape. However, the shape of the grain became irregular and the number of “petal” shape grains decreased

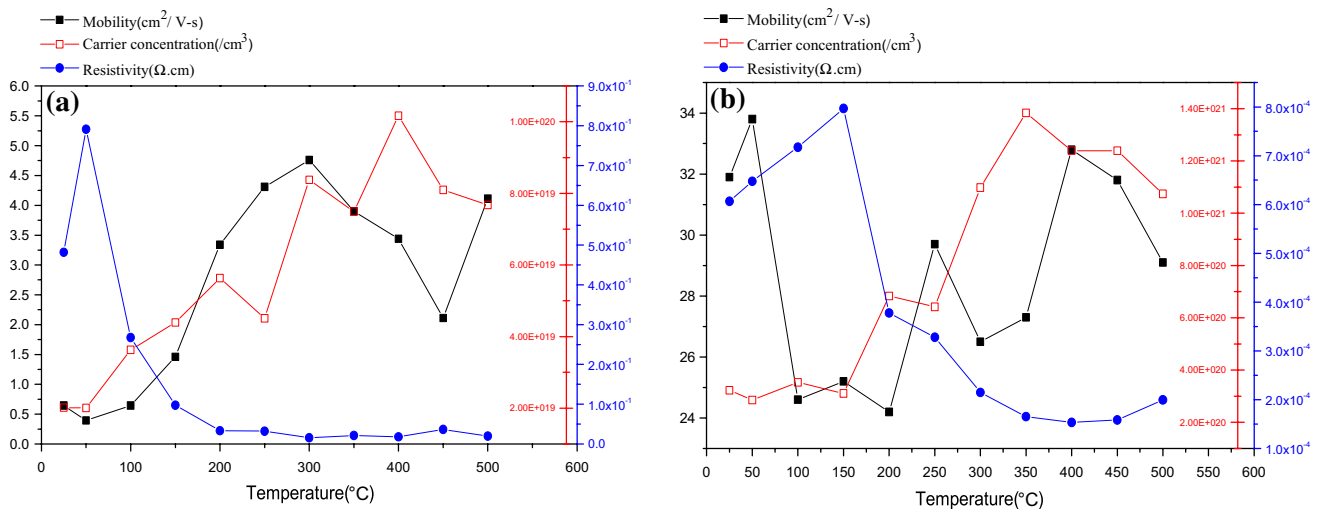
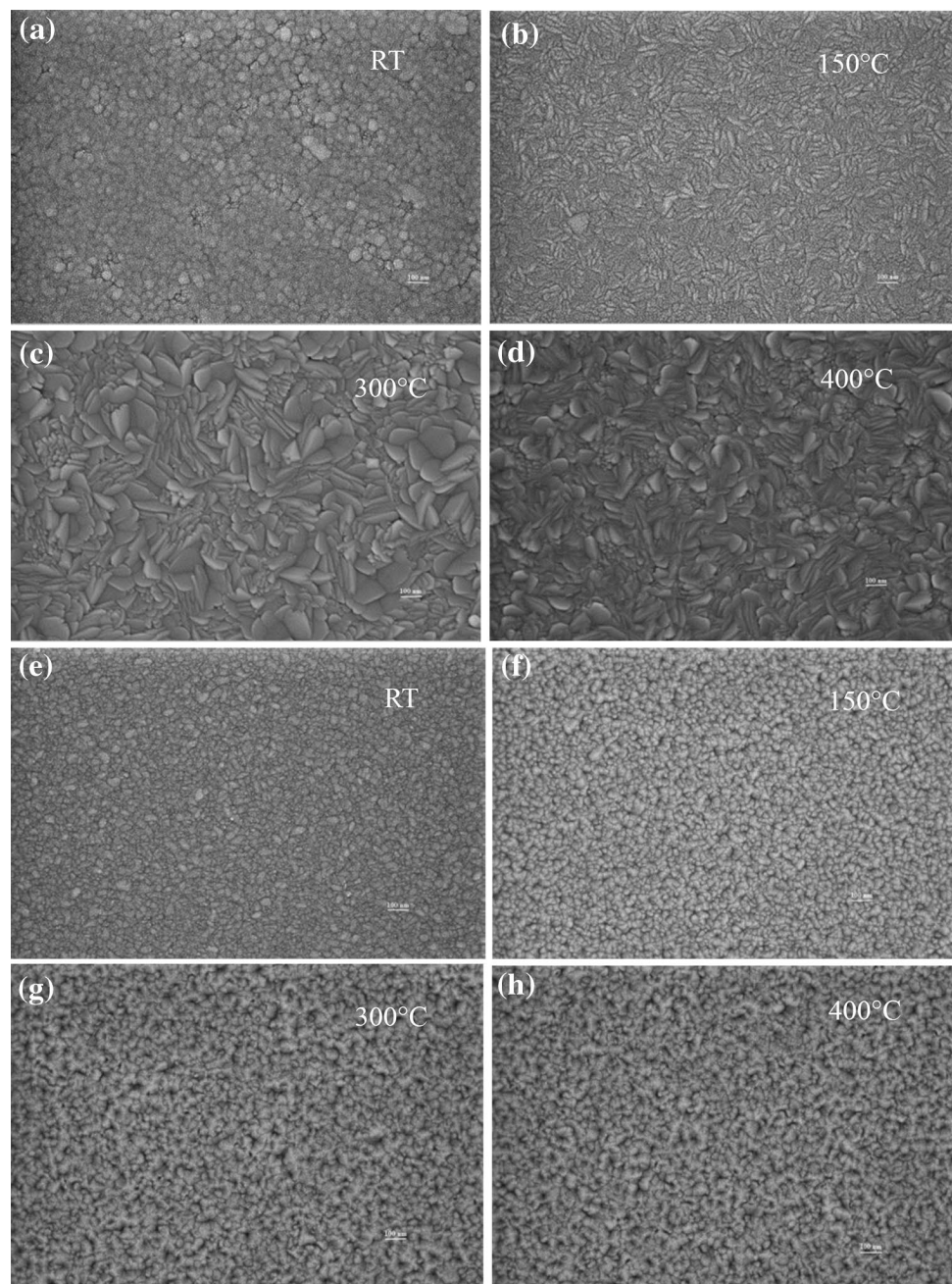


**Fig. 3** The electrical properties of **a** AZO and **b** ITO thin films prepared by the different substrate temperatures



**Fig. 4** SEM images of ITO films (a–d) and AZO films (e–h) deposited using various substrate



when the temperature exceeded 300 °C. Figure 4e–h shows the surface morphology of the AZO films deposited at different substrate temperatures. The same as the ITO films, the AZO film deposited at RT has a smooth surface with granule-shaped grains. Compared with ITO thin films, however, the crystallinity and grain size of the AZO films were barely improved as the substrate temperature increased. When the substrate temperature increased, the AZO films exhibited a small grain size and strip-shaped grains. This may be the reason for the electrical properties of the ITO films deposited at various temperatures were better than the AZO thin films.

As we all know, it is meaningful for materials used in devices [18–20]. In order to verify the effects of AZO and ITO films sputtered at different temperatures for  $\text{Cu}_2\text{ZnSnS}_4$  (CZTS) solar cells, we used these thin films as windows layer of CZTS solar cells. About 22 CZTS solar cells with these different windows layer were traditionally fabricated, and the basic fabrication process for our CZTS process has been described elsewhere [21]. According to Fig. 5, it can be concluded that the CZTS solar cells using the windows layer sputtered at more than 450 °C had no characterization of J–V properties. This may be the heating temperature is too high so that the solar cells lost performance.

Figure 5 presents the statistics data of  $V_{oc}$ ,  $J_{sc}$ , fill factor, and efficiency of the CZTS solar cells using different AZO and ITO films as windows layer, respectively. It can be seen from Fig. 5d that the mean efficiency of the solar cells with ITO films is much higher than that of AZO films. However, for both of AZO and ITO samples, the mean efficiency decreases dramatically when the substrate temperature exceeds 300 °C. The poor efficiency of CZTS solar cells with AZO or ITO films sputtered at higher substrate temperature may be attributed to the second order phase transition between ordered-kesterite and disordered-kesterite which was characterized by a critical temperature below (260 °C for CZTS) [22]. As the substrate temperature is 300 °C, the CZTS solar cells achieve the highest efficiency of 3.66% (AZO) and 5.12% (ITO), respectively. The open circuit voltage of the CZTS solar cells with AZO films is not changed obviously, but the solar cells using ITO films are opposite, as shown in Fig. 5a. The  $J_{sc}$  of the CZTS solar cells prepared by AZO or ITO films is basically invariant from RT to 300 °C, while it decreases rapidly for AZO samples and it increases slowly for ITO samples with the substrate temperature

increasing. This may be attributed to the improvement of grain sizes of ITO films sputtered at higher temperature, which consisted with SEM images of ITO films shown in Fig. 4a–d. The variation of fill factor is similar with that of efficiency, the highest fill factor is 42.37% belonging to ITO sample at 300 °C. From the results above, it can be concluded that the photovoltaic parameters of CZTS solar cells using ITO films as window layer are better than that of CZTS solar cells using AZO films, which is consistent with the previous confirmation that the electrical properties of ITO films are better than those of AZO films.

Figure 6 shows J–V characteristics of the champion CZTS thin film solar cells using AZO or ITO films as the windows layer. However, the CZTS film solar cells prepared by ITO films with the highest efficiency of 5.12% is still low mainly due to low fill factor (FF) and small  $J_{sc}$ , which may be caused by lots of defect states in the CZTS bulk and at grain boundaries [23], an imperfect pn-junction in CZTS/CdS interface [24] and relatively thick  $MoS_2$  layer [25]. All these factors will be optimized in future. Here, it should be emphasized that the CZTS thin film

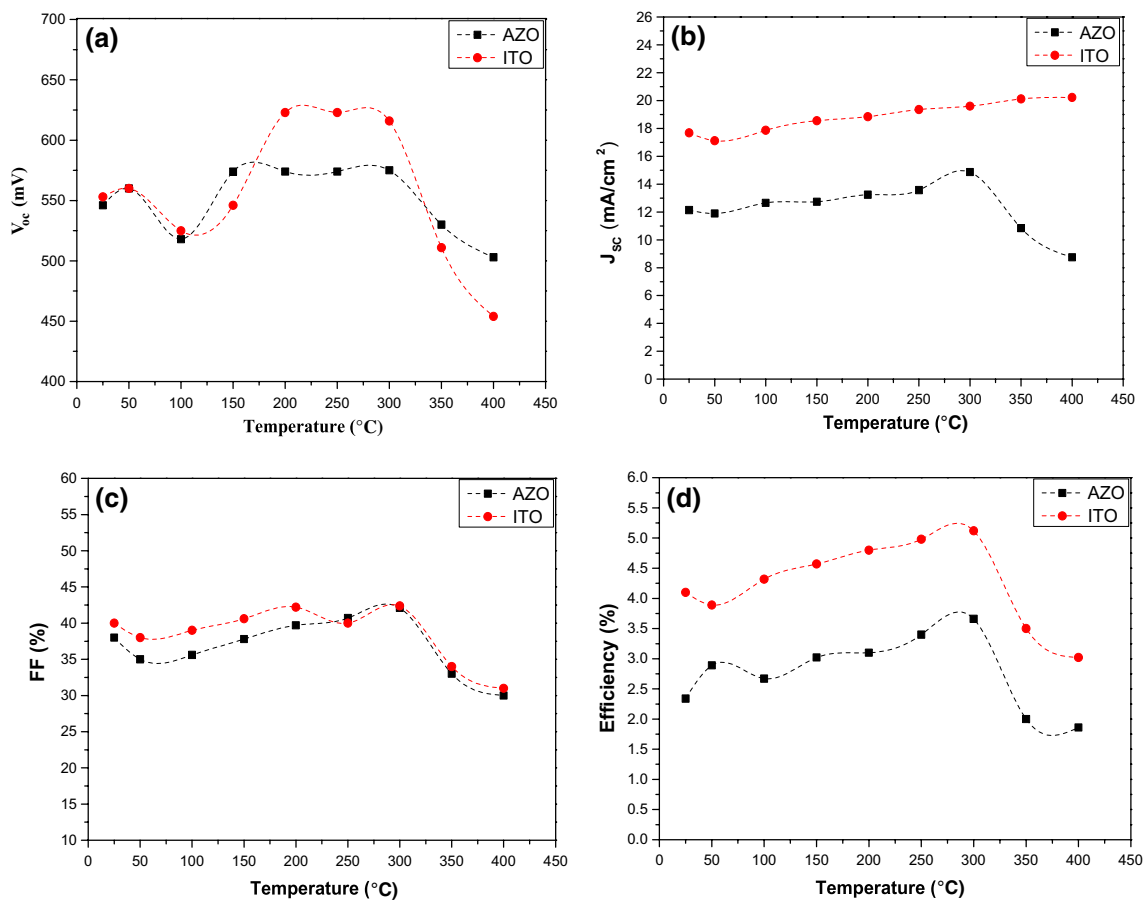


**Fig. 5** The statistics data of  $V_{oc}$  (a),  $J_{sc}$  (b), fill factor (c), and efficiency (d) of the CZTS solar cells using different AZO and ITO films as windows layer

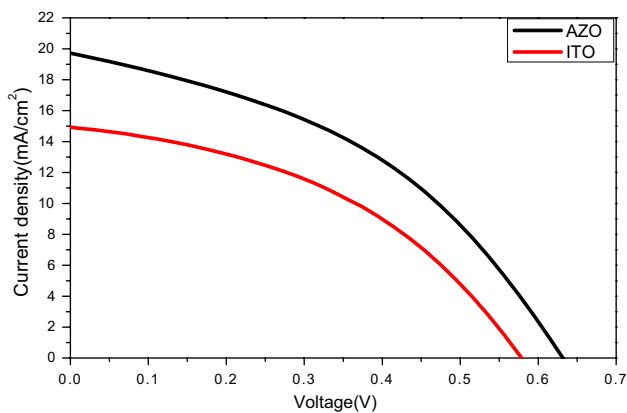


**Fig. 6** J–V characteristics of CZTS solar cells obtained by the different window layers

solar cells prepared by ITO films have better performance than that of CZTS solar cells prepared by AZO films.

## 4 Conclusions

In summary, by changing the substrate temperature, AZO and ITO thin films were prepared demonstrating different electrical and optical properties. Meanwhile, the optical band gap energies of AZO and ITO films were ranged from 3.28 to 3.48 eV and 3.33–3.92 eV, respectively. And the lowest resistivity of AZO thin films was  $1.57 \times 10^{-2} \Omega \text{ cm}$  for the substrate temperature of 300 °C. However, the lowest resistivity of ITO thin films was  $1.5 \times 10^{-4} \Omega \text{ cm}$  for the temperature of 400 °C. In addition, the surface morphologies of AZO and ITO films were also investigated. The crystallinity and grain size of the AZO films were barely improved as the substrate temperature increased, but the ITO films were opposite. Finally, CZTS solar cells were developed using AZO or ITO films as window layers. when the substrate temperature exceeds 300 °C, the photovoltaic parameters of CZTS solar cells drops rapidly, it may be owing to the second order phase transition between ordered-kesterite to disordered-kesterite. The CZTS solar cells were obtained with the highest efficiency of 3.66% (AZO) and 5.12% (ITO), respectively.

**Acknowledgements** This work was supported by Collaborate Innovation Center of Research and Development of Renewable Energy in the Southwest Area (Grant No. 05300205020516009) and the National Natural Science Foundation of China (Grant No. 61167003), also by key project of National and International Scientific and Technological cooperation (Grant No. 2011DFA62380).

## References

1. S.H. Jeong, J.H. Boo, Influence of target-to-substrate distance on the properties of AZO films grown by RF magnetron sputtering. *Thin Solid Films* **447–448**, 105–110 (2004)
2. A. Alyamani, N. Mustapha, Effects of high dose gamma irradiation on ITO thin film properties. *Thin Solid Films* **611**, 27–32 (2016)
3. P. Thilakan, C. Minarini, S. Loreti, E. Terzini, Investigations on the crystallisation properties of RF magnetron sputtered indium tin oxide thin films. *Thin Solid Films* **388**, 34–40 (2001)
4. M. Toki, M. Aizawa, Sol-gel formation of ITO thin film from a sol including ITO powder. *J. Sol-Gel. Sci. Technol.* **8**(1–3), 717–720 (1997)
5. D. Paine, T. Whitson, D. Janiac, R. Beresford, C. Yang, B. Lewis, A study of low temperature crystallization of amorphous thin film indium-tin-oxide. *J. Appl. Phys.* **85**, 8445–8450 (1999)
6. T. Maruyama, K. Fukui, Indium tin oxide films prepared by chemical vapour deposition. *Thin Solid Films* **203**(2), 297–302 (1991)
7. M.T. Wei Wang, O. Winkler, Gunawan, Device characteristics of CZTSSe thin-film solar cells with 12.6% efficiency. *Adv. Energy Mater.* **4**, 1301465 (2014)
8. S. Giraldo, T. Thersleff, G. Larramona,  $\text{Cu}_2\text{ZnSnSe}_4$  solar cells with 10.6% efficiency through innovative absorber engineering with Ge superficial nanolayer. *Prog. Photovolt. Res. Appl.* **24**, 1359–1367 (2016)
9. B. Shin, O. Gunawan, Y. Zhu, Thin film solar cell with 8.4% power conversion efficiency using an earth-abundant  $\text{Cu}_2\text{ZnSnS}_4$  absorber. *Prog. Photovolt. Res. Appl.* **21**, 72–76 (2013)
10. J. Li, H. Wang, L. Wu, Growth of  $\text{Cu}_2\text{ZnSnSe}_4$  film under controllable se vapor composition and impact of low Cu content on solar cell efficiency. *ACS Appl. Mater. Interfaces* **8**(16), 10283–10292 (2016)
11. J.W. Leem, J.S. Yu, Structural, optical, and electrical properties of AZO films by tilted angle sputtering method. *Thin Solid Films* **518**, 6285–6288 (2010)
12. D.-W. Kang, S.-H. Kuk, K.-S. Ji, H.-M. Lee, M.-K. Han, Effects of ITO precursor thickness on transparent conductive Al doped ZnO film for solar cell applications. *Solar Energy Mater. Solar Cells* **95**, 138–141 (2011)
13. H. Kartik, S.K. Patel, Rawal, Influence of power and temperature on properties of sputtered AZO films. *Thin Solid Films* **620**, 182–187 (2016)
14. H.T. Chang, G.J. Chen, Influence of nitrogen doping on the properties of ZnO films prepared by radio-frequency magnetron sputtering. *Thin Solid Films* **618**, 84–89 (2016)
15. M. Mohil, G.A. Kumar, Gamma radiation induced effects in  $\text{TeO}_2$  thin films. *J. Nano Electron. Phys.* **5**(2), 80–84 (2013)
16. C. Frisk, T. Ericson, S.Y. Li et al., Combining strong interface recombination with bandgap narrowing and short diffusion length in  $\text{Cu}_2\text{ZnSnS}_4$  device modeling. *Solar Energy Mater. Solar Cells* **144**, 364–370 (2016)
17. S. Yu, W. Yang, L. Li, W. Zhang, Improved chemical stability of ITO transparent anodes with a  $\text{SnO}_2$  buffer layer for organic solar cells. *Solar Energy Mater. Solar Cells* **144**, 652–656 (2016)
18. K.-J. Yang, J.-H. Sim, D.-H. Son, Effects of the compositional ratio distribution with sulfurization temperatures in the absorber layer on the defect and surface electrical characteristics of  $\text{Cu}_2\text{ZnSnS}_4$  solar cells. *Prog. Photovolt. Res. Appl.* **23**, 1771–1784 (2015)
19. S.G. Lee, J. Kim, H.S. Woo, Structural, morphological, compositional, and optical properties of single step electrodeposited  $\text{Cu}_2\text{ZnSnS}_4$  (CZTS) thin films for solar cell application. *Curr. Appl. Phys.* **14**, 254–258 (2014)

20. M. Dimitrievska, A. Fairbrother, E. Saucedo, Secondary phase and Cu substitutional defect dynamics in kesterite solar cells: impact on optoelectronic properties. *Solar Energy Mater. Solar Cells* **149**, 304–309 (2016)
21. Z.-S. Li, S.-R. Wang, Z. Jiang,  $\text{Cu}_2\text{ZnSnS}_4$  solar cells prepared by sulfurization of sputtered ZnS/Sn/CuS precursors. *Physica B* **502**, 56–60 (2016)
22. G. Rey, T.P. Weiss, J. Sandler, Ordering kesterite improves solar cells: a low temperature post-deposition annealing study. *Solar Energy Mater. Solar Cells* **151**, 131–138 (2016)
23. G.Y. Kim, A.R. Jeong, J.R. Kim, Surface potential on grain boundaries and intragrain of highly efficient  $\text{Cu}_2\text{ZnSn(S,Se)}_4$  thin-films grown by two-step sputtering process. *Solar Energy Mater. Solar Cells* **127**, 129–135 (2014)
24. M. Neuschitzer, Y. Sanchez, S. López-Marino, H. Xie, A. Fairbrother, M. Placidi, S. Haass, V. Izquierdo-Roca, A. Perez-Rodriguez, E. Saucedo, Optimization of CdS buffer layer for high-performance  $\text{Cu}_2\text{ZnSnSe}_4$  solar cells and the effects of light soaking: elimination of crossover and red kink. *Prog. Photovolt. Res. Appl.* **23**, 1660–1667 (2015)
25. S.W. Shin, K.V. Gurav, C.W. Hong, Phase segregations and thickness of the  $\text{Mo(S,Se)}_2$  layer in  $\text{Cu}_2\text{ZnSn(S,Se)}_4$  solar cells at different sulfurization temperatures. *Solar Energy Mater. Solar Cells* **143**, 480–487 (2015)